WL-EMP-IN-100

Interaction Notes

Note 100

10 April 1972

Induced Electric Currents on Some Configurations of Wires

Part II

Non-perpendicular Intersecting Wires

conductors, thin wires, transmission lines

Terry T. Crow
Thomas H. Shumpert
Mississippi State University
State College, Mississippi 39762

Clayborne D. Taylor
University of Mississippi
University, Mississippi 38677

Induced Electric Currents on Some Configurations of Wires

Part II

Non-perpendicular Intersecting Wires

ABSTRACT

The general equations previously developed for a system of thin conducting wires in an arbitrary geometry are applied to a planar set of three non-orthogonal wires.

FOREWORD

Figures presenting numerical results are grouped at the end of the report. Appendix I outlines one approach by which thin-wire theory might be modified to deal with thick structures. We wish to thank Dr. Carl Baum and Capt P. R. Barnes for their interest and suggestions during the course of this work.

1. Introduction

High speed digital computers have made possible the theoretical study of certain classes of electromagnetic problems for arbitrary configurations of conducting wire structures. Coupled integral equations predicting electric currents induced on these wires by arbitrary incident fields have been developed [1,2,3,4,5]. For an N-wire system the number of coupled integral equations to be solved will be N. If the wires intersect, additional unknowns are introduced and these necessitate additional boundary conditions - the Kirchhoff current law and the continuity of the scalar potential [2].

2. Discussion

The particular case of interest in this paper is a three wire system having the configuration shown in Figure 1. This system is a second stage -

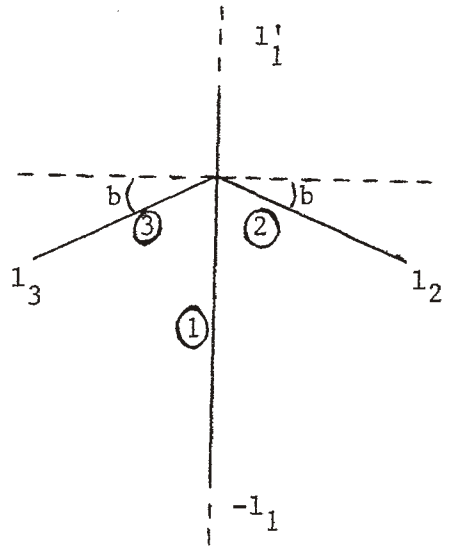

Figure 1. Three Wire Configuration

the first being a treatment of perpendicular crossed wires [3] - in the development of a realistic model of an aircraft and its behavior as a scattering

antenna. The treatment of the configuration shown in Figure 1 is general in that the various length parameters and the sweep angle, b, can be varied. Wires 2 and 3 are assumed to be the same length ($l_2 = l_3$) and the similarity to an aircraft wing-fuselage structure becomes obvious. Thus the structure contains an electromagnetic symmetry plane [6].

The system of coupled integral equations applied to this three wire system becomes

$$\sum_{m=1}^{3} \int_{Lm} dS'_m \, I_m(S'_m)\pi(S_n,S'_m) = C_n \cos kS_n + D_n \sin kS_n$$

$$-j \frac{4\pi}{\eta} \int_o^{S_n} dS'_n \, E^i_{S_n}(S'_n) \sin k(S_n-S'_n) \qquad (1)$$

where n=1,2,3 and $\eta = \sqrt{\mu/\varepsilon}$. $E^i_{S_n}$ is the component of the incident field in the direction of S_n and $\pi(S_n,S'_m)$ is defined as

$$\pi(S_n,S'_m) = (\hat{S}'_m \cdot \hat{S}_n) \, G(S_n,S'_m)$$

$$- \int_o^{S_n} dS'_n \cos k(S_n-S'_n) \, \Psi(S'_n,S'_m) \qquad (2)$$

where

$$\Psi(S'_n,S'_m) = \frac{\partial}{\partial S'_m} G(S'_n,S'_m) + G(S'_n, S'_m) \frac{\partial}{\partial S'_n} (\hat{S}'_m \cdot \hat{S}'_n)$$

$$+ (\hat{S}'_m \cdot \hat{S}'_n) \frac{\partial}{\partial S'_n} G(S'_n,S'_m) \qquad (3)$$

The unit vectors associated with the wires numbered ① → ③ in Figure 1 are, respectively

$$\hat{S}_1 = \hat{j}$$

$$\hat{S}_2 = \hat{i} \cos b - \hat{j} \sin b$$

$$\hat{S}_3 = -\hat{i} \cos b - \hat{j} \sin b$$

The Green's functions are of the form

$$G(S_i, S_j') = \frac{\exp[-jkR(S_i, S_j')]}{R(S_i, S_j')}$$

with

$$R(S_1, S_1') = [(S_1 - S_1')^2 + a_1^2]^{\frac{1}{2}}$$

$$R(S_j, S_j') = [(S_j - S_j')^2 + a_2^2]^{\frac{1}{2}} \quad j = 2,3$$

$$R(S_1, S_j') = [S_1^2 + 2S_1 S_j' \sin b + S_j'^2 + a_1^2]^{\frac{1}{2}} \quad j = 2,3$$

$$R(S_j, S_1') = [S_j^2 + 2S_1' S_j \sin b + S_1'^2 + a_2^2]^{\frac{1}{2}} \quad j = 2,3$$

$$R(S_2, S_3') = [S_2^2 + 2S_2 S_3' \cos 2b + S_3'^2 + a_2^2]^{\frac{1}{2}}$$

$$R(S_3, S_2') = [S_3^2 + 2S_3 S_2' \cos 2b + S_2'^2 + a_2^2]^{\frac{1}{2}}$$

where a_1 is the radius of wire 1 and a_2 is the radius of wires 2 and 3.

The remaining undefined terms in (1) are the integrals involving the field expressions. For a single incoming plane wave directed toward the

origin from the $z > 0$ space and in the θ, ϕ direction - these are the usual polar angles - two polarizations are considered: $\vec{E}$ in the x,y plane (E-polarization) and $\vec{H}$ in the x,y plane (H-polarization). To illustrate a specific example the incident field along wire 2 for E-polarization is

$$E^i_{S_2}(S_2') = E_o[\cos\alpha \cos b - \sin\alpha \sin b]\, x$$

$$\exp\left[jkS_2'(\sin\theta\cos\phi\cos b - \sin\theta\sin\phi\sin b)\right] \qquad (4)$$

α is the polarization angle for E^i and is arbitrarily assigned such that $\alpha = \phi + \pi/2$, while E_o is the magnitude of the incident plane wave. For H-polarization the exciting field along wire 2 is

$$E^i_{S_2}(S_2') = E_o[\sin\beta \cos\gamma \cos b - \sin\beta \sin\gamma \sin b]\, x$$

$$\exp\left[jkS_2'(\sin\theta\cos\phi\cos b - \sin\theta\sin\phi\sin b)\right] \qquad (5)$$

and the polarization angles are arbitrarily defined to be $\beta=\theta+\pi$, $\gamma=\phi$. Similar expressions can be found for the other wires in the system.

3. Numerical Results

In the actual analysis of the behavior of structures, the incoming plane wave of interest is considered to be composed of a symmetric portion and an antisymmetric portion whose sum reproduces the single incoming wave. The analysis is thus presented in terms of four cases: E-polarization, symmetric and antisymmetric; H-polarization, symmetric and antisymmetric (see Figures 2 and 3).

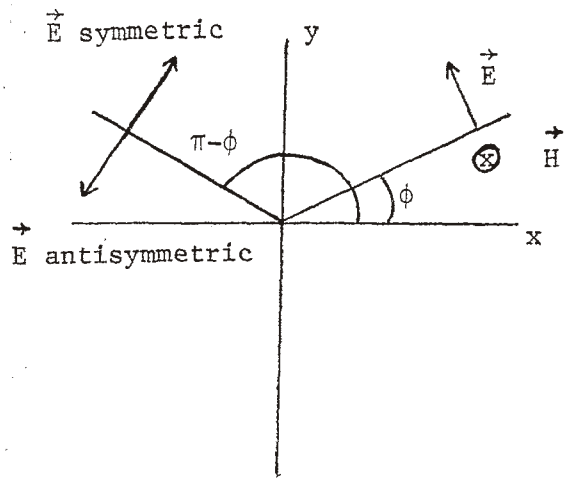

Figure 2. E-Polarization Modes

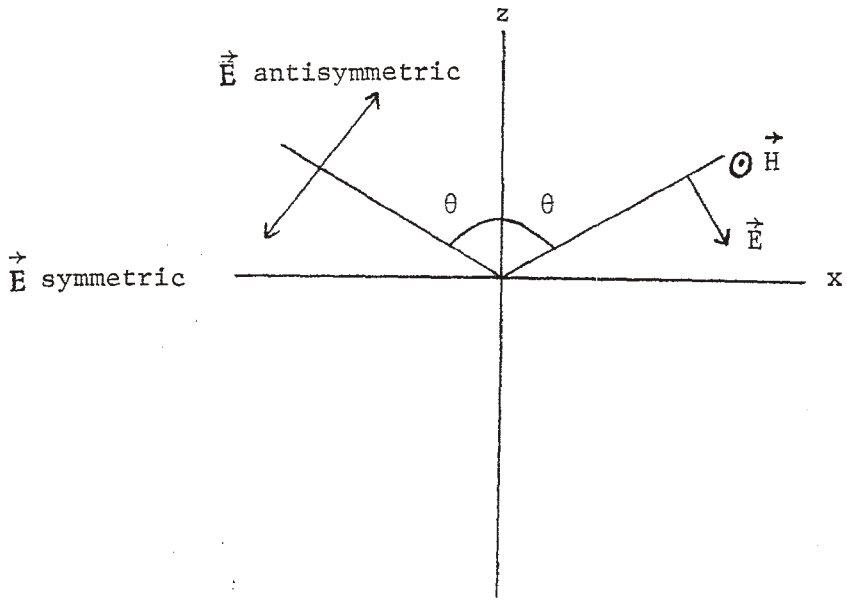

Figure 3. H-Polarization Modes

The treatment of a single incoming plane wave, amplitude E, at arbitrary angles of incidence (θ,ϕ) and arbitrary polarization proceeds in the following way. First, the E vector of the incoming wave is resolved into a component in the x,y plane (E-pol.) and a component perpendicular to $\vec{k}$ and the just defined E-polarization part. This now defines an E-polarization incoming wave, amplitude E_E, and an H-polarization incoming wave, amplitude E_H. Each of these waves is now resolved into symmetric and antisymmetric parts, each

having magnitude $E_E/2$ for E-polarization and $E_H/2$ for H-polarization. Numerical results are presented in the form of currents and linear charge densities normalized by $2l_2$ and E_0 where E_0 is the amplitude of a single incoming wave and would be equal to $E_E/2$ or $E_H/2$ as the case may be. Thus for E-polarization the exciting field along wire 2 due to two incident waves (one at θ,ϕ; the other at $\theta,\pi-\phi$) and each having amplitude E_0 becomes

$$E^i_{S_2}(S_2') = [\text{Eq. } 4] + E_0 \left\{ [\cos\Delta \cos b - \sin\Delta \sin b] \times \right.$$

$$\left. \exp j k S_2' [\sin\theta \cos(\pi-\phi) \cos b - \sin\theta \sin(\pi-\phi) \sin b] \right\} \qquad (6)$$

and the symmetric and antisymmetric fields will be given by setting $\Delta = \pi/2-\phi$ and $\Delta = 3\pi/2-\phi$ in that order. The remaining five field expressions (E-pol. on wires 1 and 3 and H-pol. on all wires) can be derived in a similar manner.

The numerical analysis is based on assuming the currents to be piecewise constant within a given zone of the structure [7]. There results from this assumption a series of linear equations. The matrix form of the equations is

$$\pi F = \Gamma$$

where F is a column vector whose elements are the current magnitudes in the various zones and the C_n's and D_n's. Most elements of the (square) π matrix are derived from the integral expressions on the left side of (1) and Γ is a column vector determined from the integrals in (1) containing the incident field expressions.

Thus, the solutions of (1) provide a set of induced currents on the wire structure for a given incident, harmonic plane wave excitation. From

the currents the charge densities at various locations can be determined by use of the equation of continuity. The problem of interest is a determination of induced currents and charge densities when the structure is excited by some type of time-dependent pulse. To obtain such results a series of frequency values are run and the desired results are obtained by performing the necessary Fourier inversion for the given incoming pulse.

4. Graphical Presentation

All data presented on the following figures are for the case

$$1_1'/1_1 = 0.5 \quad 21_2/(1_1+1_1') = 1.0 \quad 21_2/a = 20.0$$

$$a_1 = a_2 = a$$

This physical structure has been studied for $b = 0^o$ in a previous note [3]. In this report, numerical results are presented for selected values of $k1_2$, normal incidence, and at $b = 5^o$ and $b = 30^o$. In any problem with normal incidence, E-polarization refers to an incoming plane wave whose E vector is parallel to wire 1 while H-polarization refers to an incoming plane wave whose E vector is in the plane of the 3-wire structure and perpendicular to wire 1.

In order to interpret Figures 4-19 without reference to the previous work [3], the following arguments are repeated. All curves are for incoming plane waves of amplitude E_o v/m. For normal incidence there are two waves as in every angle case, and the rules of section 3 must be followed to determine the effects of a single plane wave noting that E antisymmetric and H symmetric currents are always zero for normal incidence. Figures 4-13 represent the currents at various locations on the structure as functions of $k1_2$.

In these figures the solid and dotted curves represent the magnitudes and phases of the currents for b = 0^{o}, while the individual points represent the magnitudes of the currents for the two angles, b = 5^{o} and b = 30^{o}. To exhibit explicitly the manner in which these data might be applied to specific problems, consider the determination of the junction current on wire 2 for kl_2 = 1.15, a single incoming plane wave of amplitude 1 v/m, E-polarization, and b = 0^{o}. This incoming wave will be synthesized from an E symmetric component, amplitude 0.5 v/m, and an E antisymmetric component, amplitude 0.5 v/m. From Figure 4, the magnitude of $I/(2l_2E_o)$ is 0.0117 amperes/volt, the phase is 0^{o}, and the (dimensionless) electrical length is 1.15. Thus, for a structure of unit length ($2l_2$ = 1m) and E_o = 0.5 v/m, the complex junction current on wire 2 is (remembering the antisymmetric contribution is zero) I = (5.85 + j 0) ma. Figure 5 represents the complex currents on wire 2 at a position one-third of the way from the junction to the end of wire 2. Other locations are similarly defined. Figures 14-19 represent the linear charge densities, λ (coulombs/meter), on various parts of the structure as functions of kl_2 and b for the system depicted in Figure 1.

APPENDIX I

Modifications for Thick Structures

The kernels appearing in the system of coupled integral equations (1) are given by (2) and (3). However these kernels are strictly valid only for thin wires. When thick structures are treated additional considerations must be made. Furthermore the boundary condition used for the current distribution is valid only for infinitesimally thin cylindrical shells. Therefore in an effort to maintain this boundary condition for thick structures the intersecting wires are considered to be open-ended cylindrical shells that may be thick.

For an open-ended cylindrical shell in free space the exact integral equation for the current distribution is [8]

$$\int_h dS'\ I(S')\ \pi\ (S,S') = C \cos kS + D \sin kS$$

$$-j\ \frac{4\pi}{\eta} \int_o^S dS'\ E_S'\ (S')\ \sin k\ (S-S') \qquad \text{(A1)}$$

where

$$\pi\ (S,S') = \frac{1}{2\pi} \int_{-\pi}^{\pi} \frac{e^{-jkR(\phi,S-S')}}{R(\phi,S-S')}\ d\phi \qquad \text{(A2)}$$

$$R(\phi,S-S') = [4a^2 \sin^2\phi/2 + (S-S')^2]^{\frac{1}{2}} \qquad \text{(A3)}$$

or

$$\pi\ (S,S') = -\frac{j}{2}\int_{-\infty}^{\infty} J_o\ (\beta a)\ H_o^{(2)}(\beta a)\ e^{j\alpha(S-S')}\ d\alpha \qquad \text{(A4)}$$

$$\beta = [k^2 - \alpha^2]^{\frac{1}{2}} \qquad \text{(A5)}$$

with the foregoing integral taken in the complex plane of α along the real axis from $-\infty$ to $+\infty$ with a downward indentation at $\alpha = -k$ and an upward indentation at $\alpha = +k$. Further information on the evaluation of A4 may be found in Appendix C of [9].

Since the coupling contribution to the wire currents is a second order effect then the approximate formulation for thin intersecting wires may be modified to treat thick cylindrical shells by using (A2) in the self-coupling terms and (2) - (3) in the cross-coupling terms. That is, for $n \neq m$ $\pi\ (S_n,S_m')$ is given by (2) but for $n = m$ use

$$\pi\ (S_n,S_n') = \frac{1}{2\pi}\int_{-\pi}^{\pi} \frac{e^{-jkR(\phi,S_n-S_n')}}{R(\phi,S_n-S_n')}\ d\phi \qquad \text{(A6)}$$

where

$$R(\phi,S-S') = [4a^2\ \sin^2\ \phi/2 + (S_n-S_n')^2]^{\frac{1}{2}} \qquad \text{(A7)}$$

or

$$\pi(S_n,S_n') = -\frac{j}{2}\int_{-\infty}^{\infty} J_o\ (\beta a_n)\ H_o^{(2)}\ (\beta a_n)\ e^{j\alpha(S_n-S_n')}\,d\alpha \qquad \text{(A8)}$$

REFERENCES

1. K. K. Mei, "On the Integral Equations of Thin Wire Antennas," IEEE Trans. Ant. Prop., Vol. AP-13, No. 3, 1965, pp 374-378.
2. C. D. Taylor, Shiow-meei Lin, and H. V. McAdams, "Electromagnetic Scattering from Arbitrary Configurations of Wires, Interaction Note 42, 15 Nov. 1968 (also IEEE Trans. Ant. Prop., Vol. AP-17, No. 5, 1969, pp 662-663).
3. C. D. Taylor and T. T. Crow, "Induced Electric Currents on Some Configurations of Wires," Part I, Interaction Note 85, Nov., 1971.
4. C. D. Taylor, Shiow-meei Lin, and H. V. McAdams, "Electromagnetic Scattering from Arbitrary Configurations of Wires, Interaction Note 42, 15 Nov. 1968 (also IEEE Trans. Ant. Prop., Vol. AP-18, no. 1, 1970, pp 133-136).
5. Shiow-meei Lin, "Electromagnetic Scattering from Thin Wire Structures of Arbitrary Configurations," Interaction Note 47, May, 1968.
6. C. E. Baum, "Interaction of Electromagnetic Fields with an Object which has an Electromagnetic Symmetry Plane," Interaction Note 63, March, 1971.
7. R. F. Harrington, Field Computation by Moment Methods, New York. The Macmillan Company, 1968.
8. R. H. Duncan and F. A. Hinchey, "Cylindrical Antenna Theory," Sandia Laboratories Technical Report SCTM 367-59-(14), July, 1959.
9. R. H. Duncan and F. A. Hinchey, "Cylindrical Antenna Theory," J. Res. NBS 64D (Radio Prop.), no. 5, 569-594, 1960.

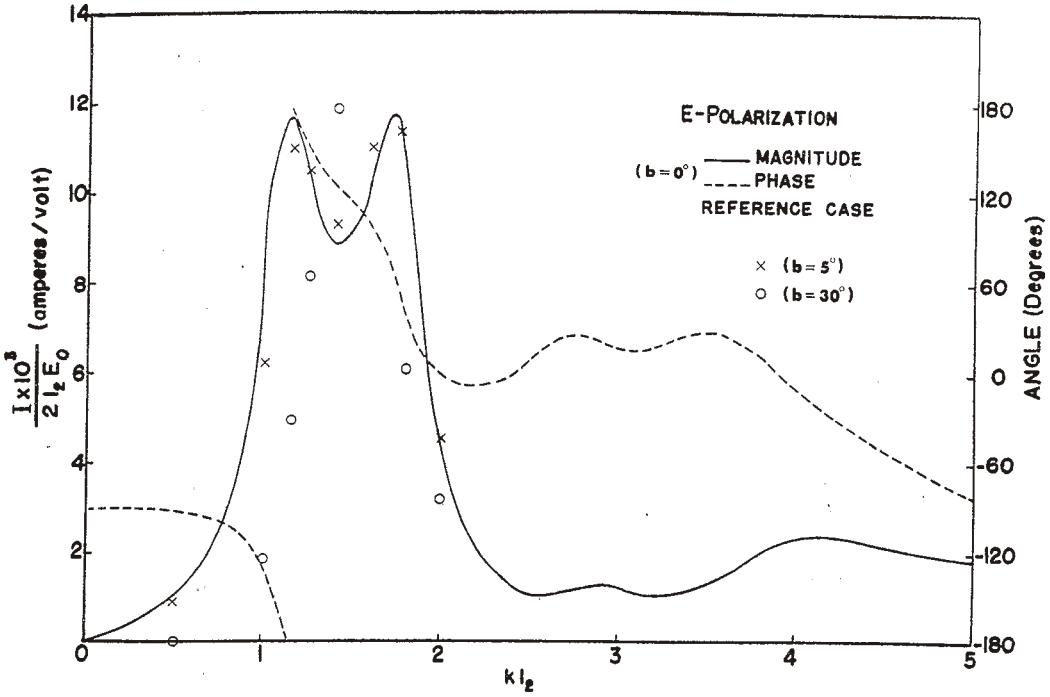

FIGURE 4. Junction current on wire 2 vs kl_2

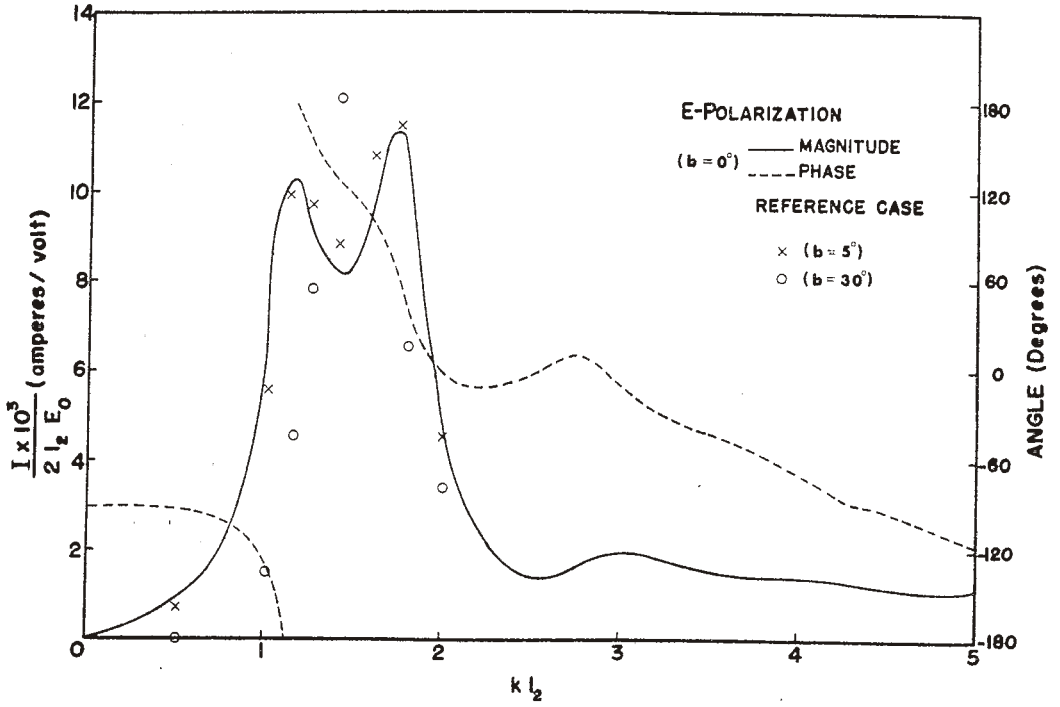

FIGURE 5. Current on wire 2 at 0.333 l_2 vs kl_2

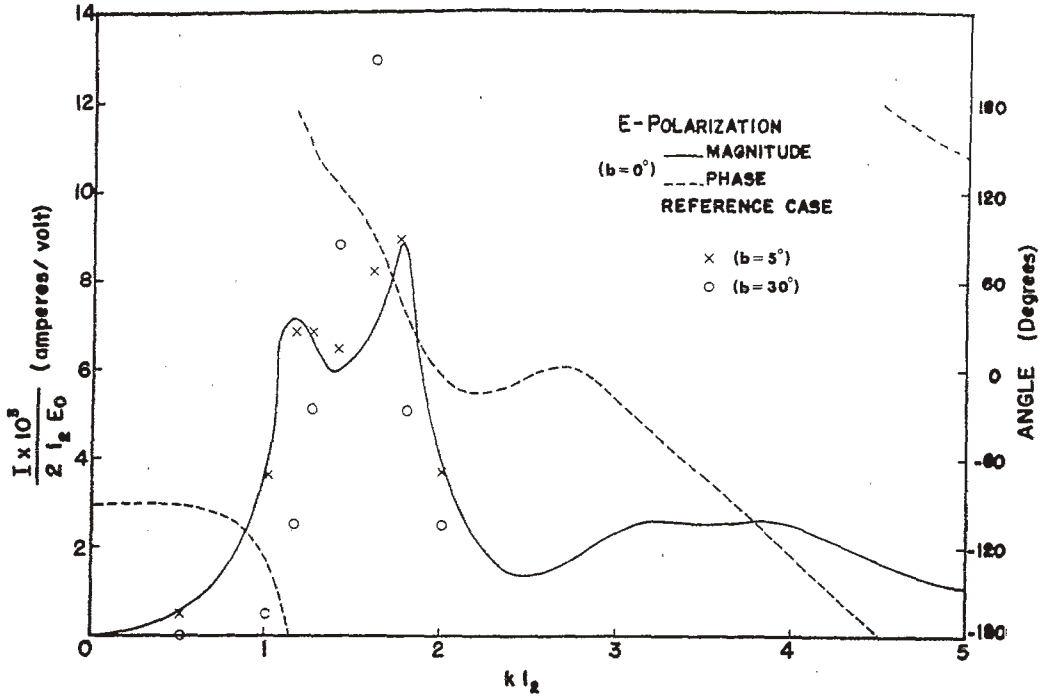

FIGURE 6. Current on wire 2 at 0.667 l_2 vs kl_2

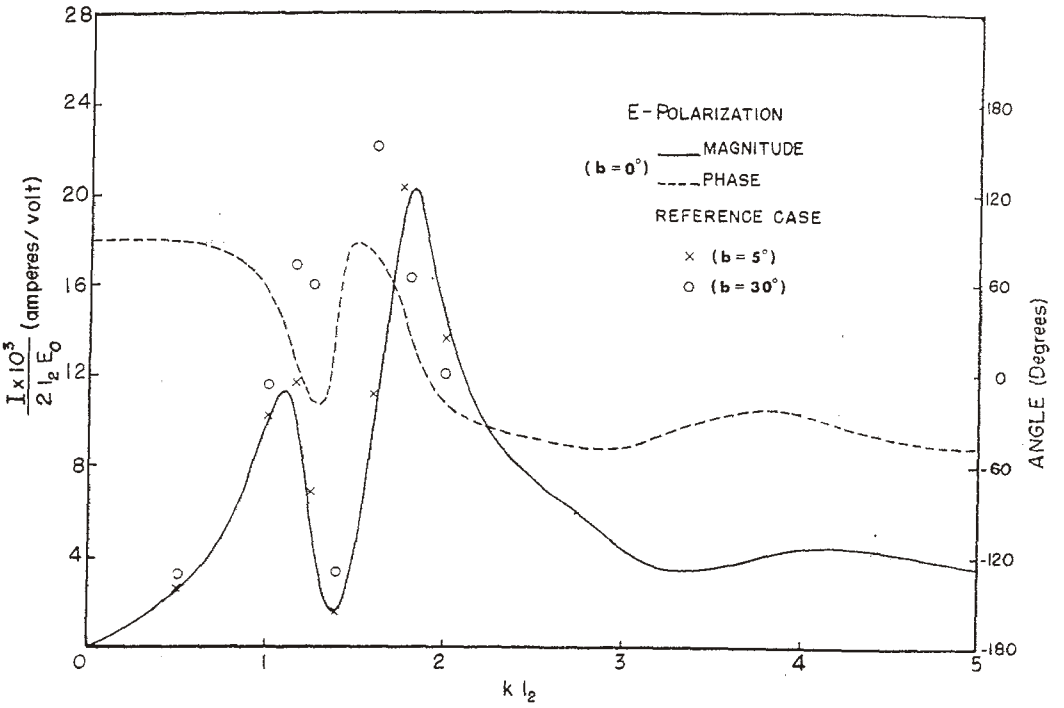

FIGURE 7. Junction current ($y=0^+$) on wire 1 vs kl_2

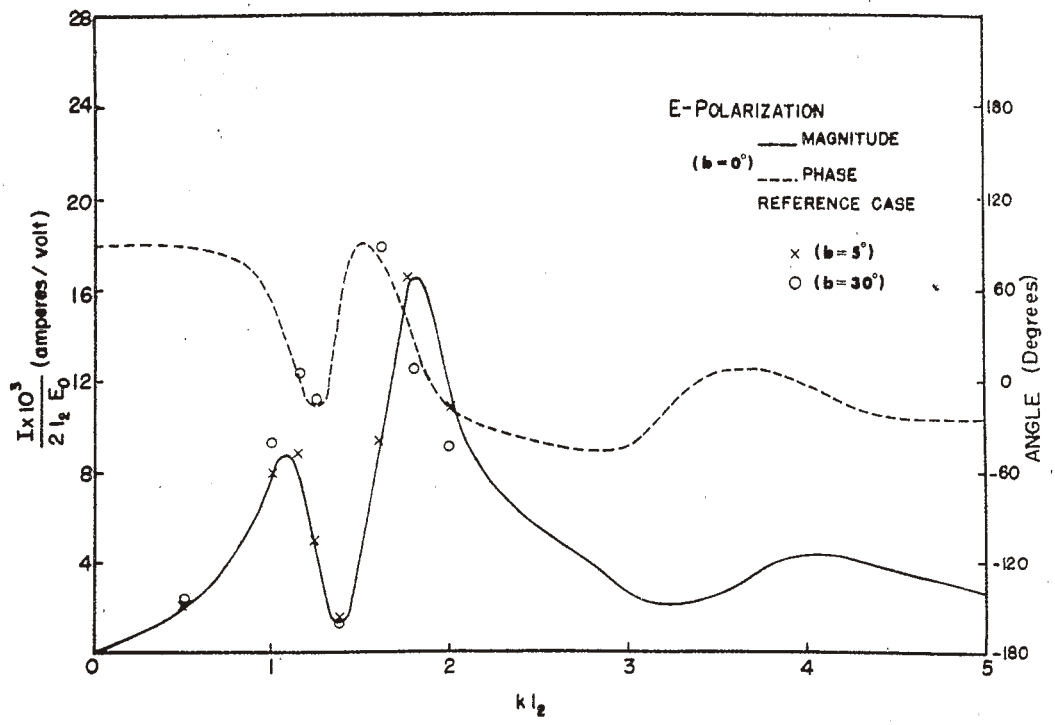

FIGURE 8. Current on wire 1 at 0.50 l_1' vs kl_2

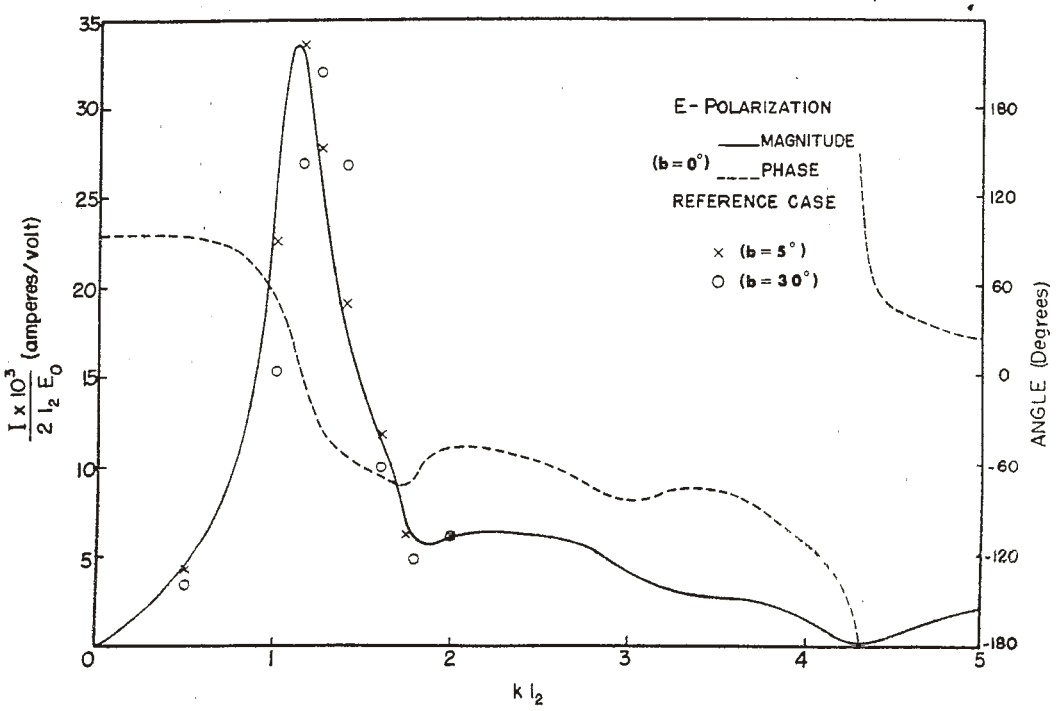

FIGURE 9. Junction current ($y=0^-$) on wire 1 vs kl_2

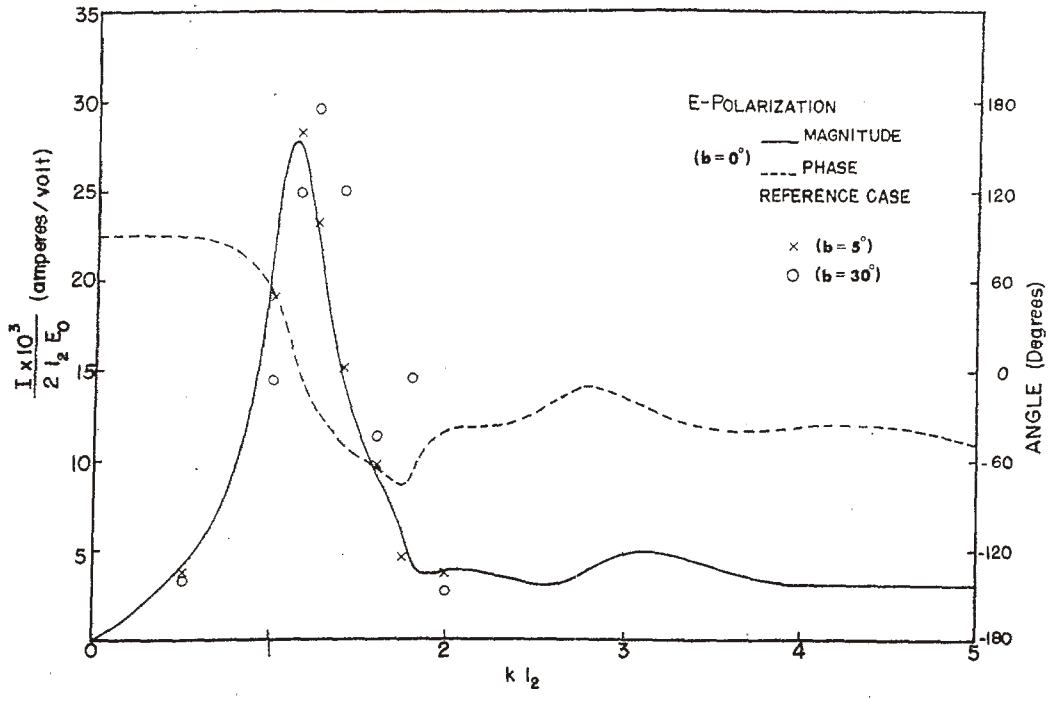

FIGURE 10. Current on wire 1 at -0.5 l_1 vs kl_2

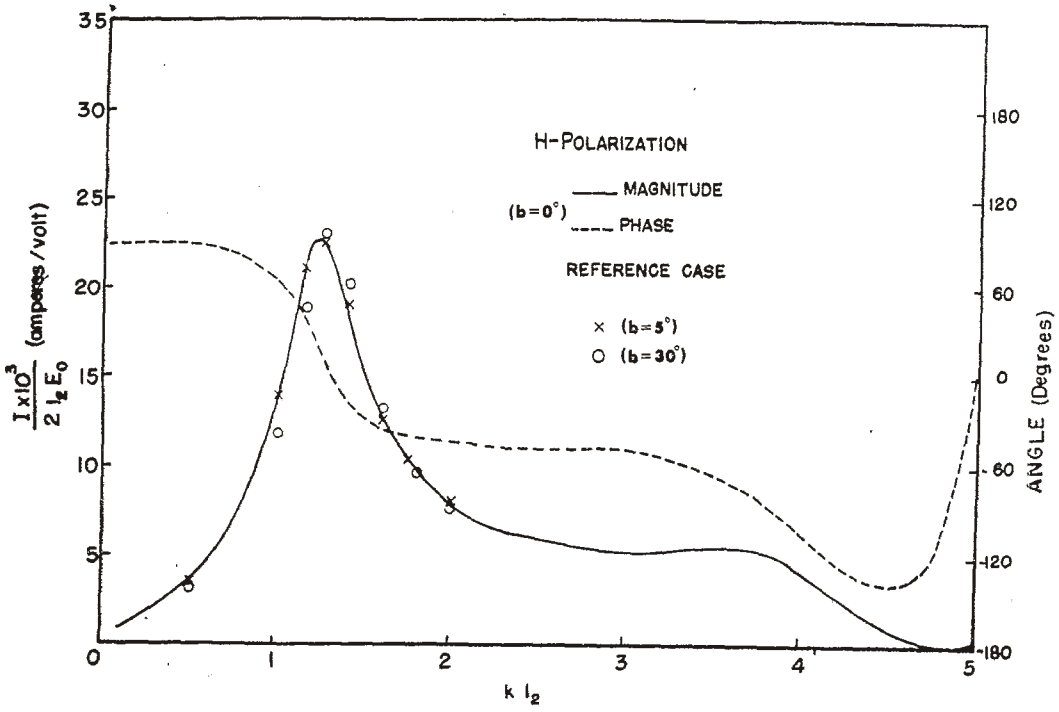

FIGURE 11. Junction current on wire 2 vs kl_2

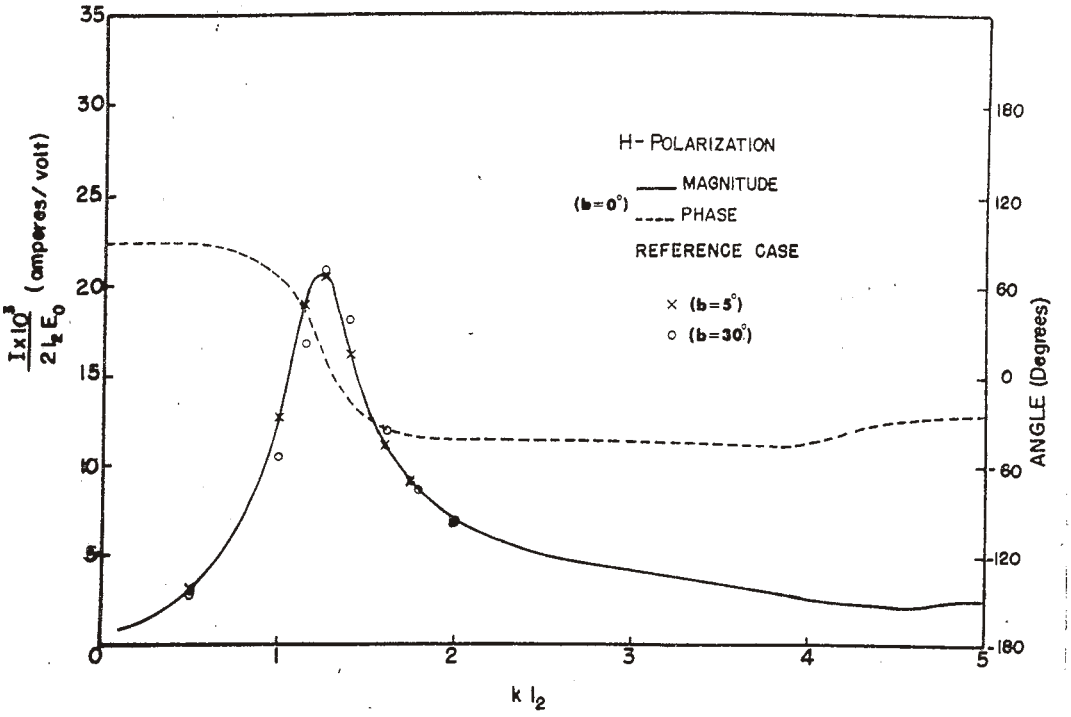

FIGURE 12. Current on wire 2 at 0.333 l_2 vs kl_2

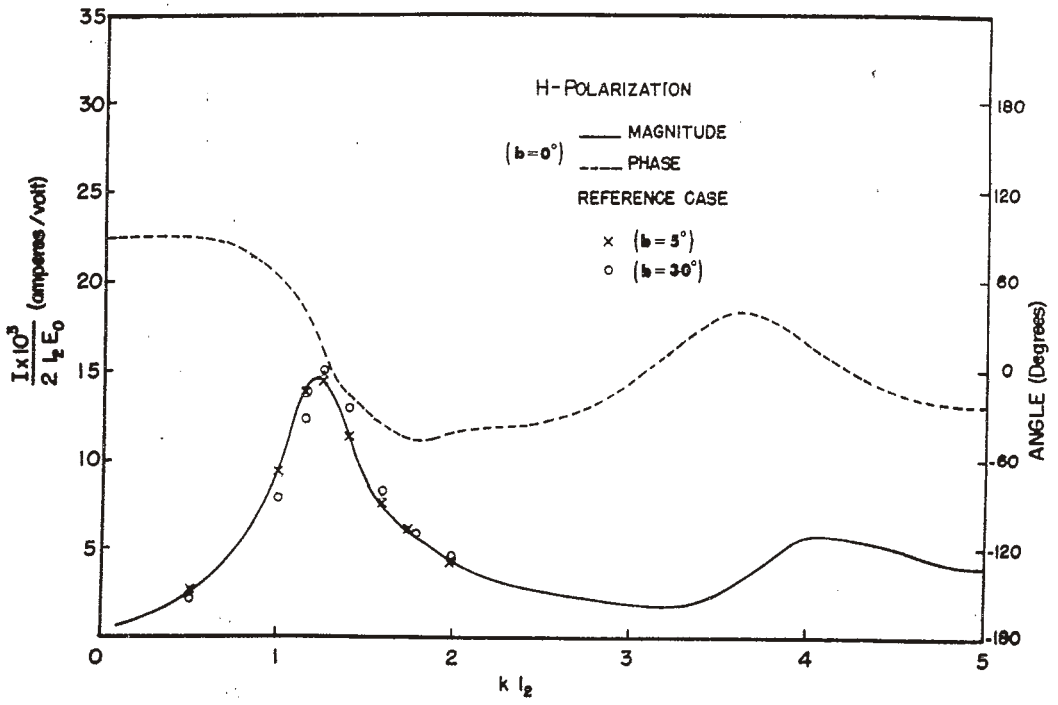

FIGURE 13. Current on wire 2 at 0.667 l_2 vs kl_2

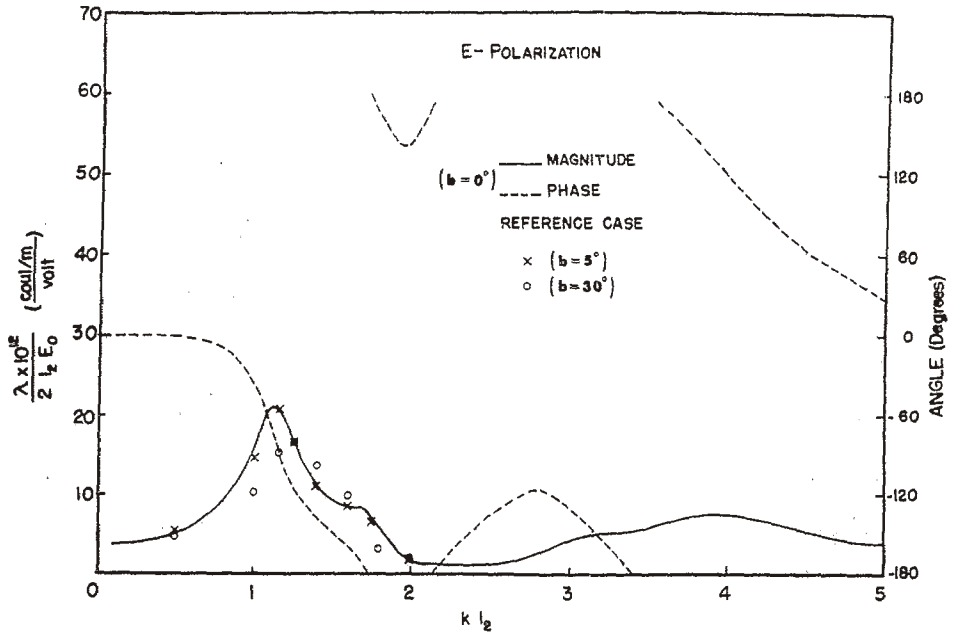

FIGURE 14. Linear charge density on wire 2 at 0.333 l_2 vs kl_2

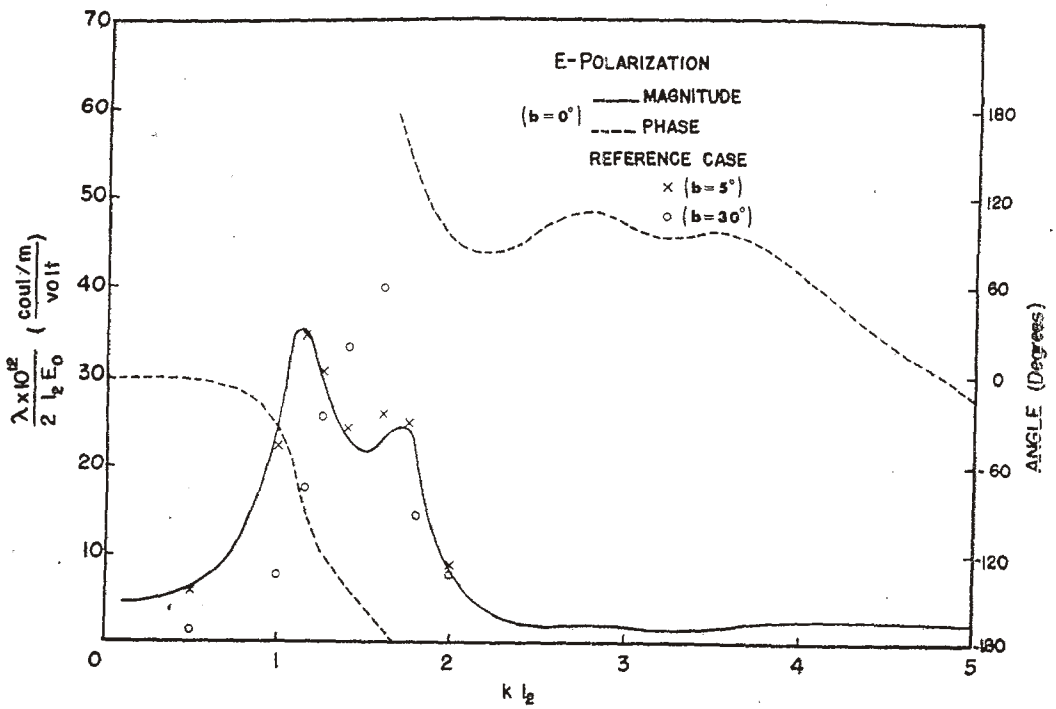

FIGURE 15. Linear charge density on wire 2 at 0.667 l_2 vs kl_2

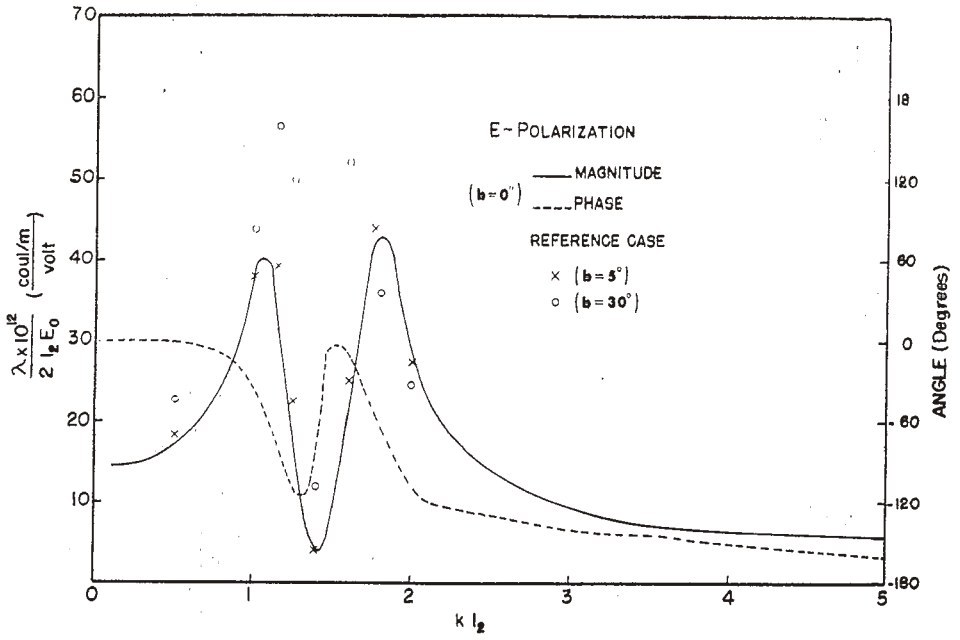

FIGURE 16. Linear charge density on wire 1 at 0.50 l_1' vs kl_2

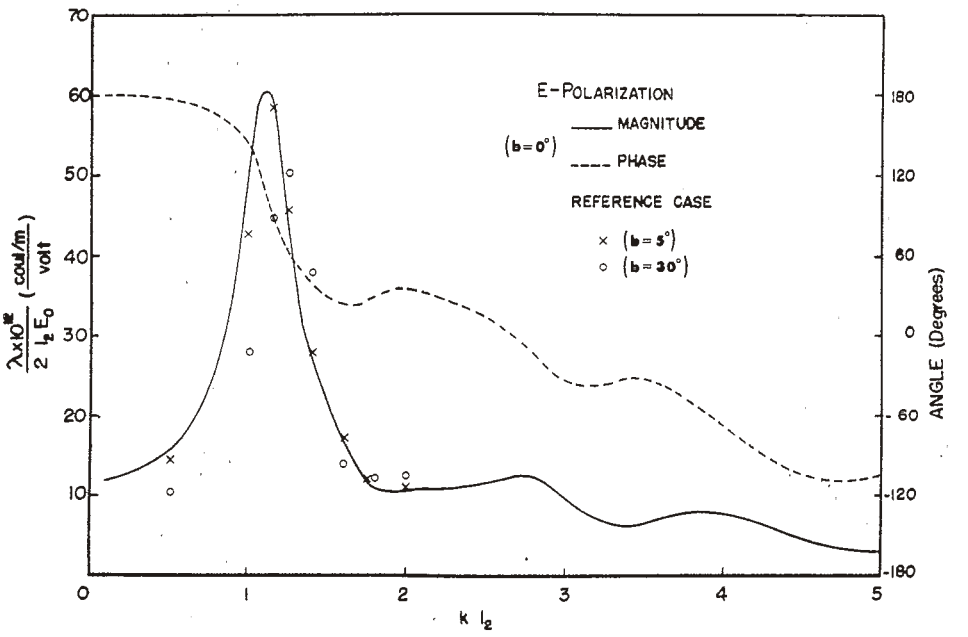

FIGURE 17. Linear charge density on wire 1 at -0.50 l_1 vs kl_2

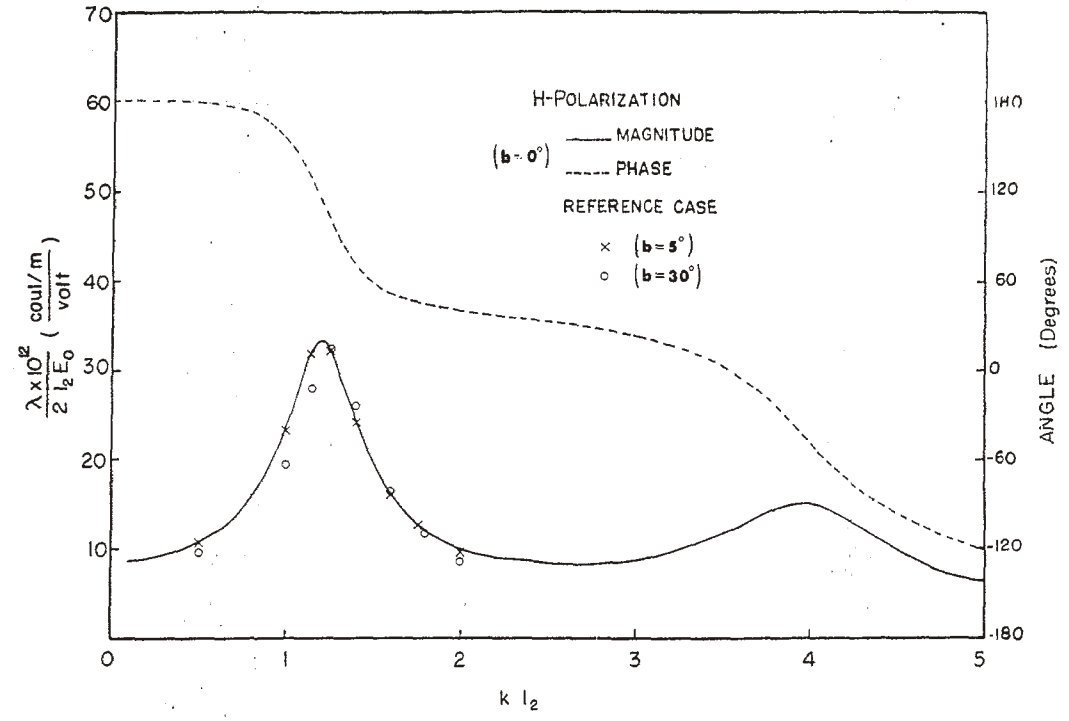

FIGURE 18. Linear charge density on wire 2 at 0.333 l_2 vs kl_2

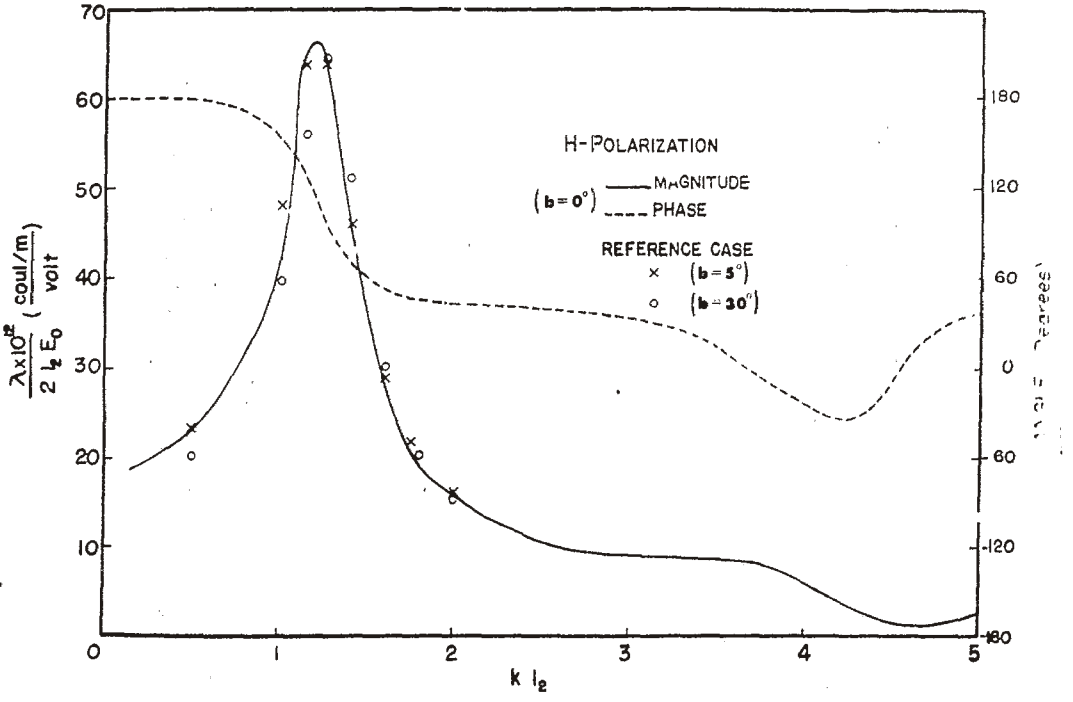

FIGURE 19. Linear charge density on wire 2 at 0.667 l_2 vs kl_2